REALISTIC MODELS OF QUANTUM DEVICES

John H. Davies, John A. Nixon and Michael J. Laughton
Department of Electronics and Electrical Engineering, Glasgow University, Glasgow, G12 8QQ, U.K.

Harold U. Baranger
AT&T Bell Laboratories, 600 Mountain Avenue, Murray Hill, NJ 07974, U.S.A.

Abstract

We have studied a realistic model of a simple quantum-mechanical device, the quantum point contact (QPC). It includes a patterned gate on the surface and the randomly-distributed donors that provide the electrons. The potential in the 2DEG is found self-consistently and conduction at the Fermi energy is analyzed quantum mechanically. There is a strong, but slowly varying, random potential. It scatters electrons between subbands even in good QPCs; quantization is preserved because scattering is predominantly forward. Quantization breaks down due to back-scattering when the length of the QPC exceeds the correlation length of the random potential, around $\frac{1}{4}\mu$m, and the characteristics reflect the detailed configuration of impurities near the QPC. Resonances trapped in bulges in the QPC cause strong back-scattering and reduce the mean free path an order of magnitude below that given by the Born approximation. Thus electrons in quantum wires have poor mobilities, not enhanced values. Some of the traditional assumptions of device modelling fail under these conditions: there is strong variation from device to device, and successive scattering events cannot be treated as independent. Genuinely quantitative modelling is hampered by our poor understanding of surface states and donors at low temperature.

1. INTRODUCTION

Advances in technology have made mobilities of 100 $m^2\ V^{-1}\ s^{-1}$ widely available for electrons trapped in a two-dimensional electron gas (2DEG) at an interface between GaAs and $Al_xGa_{1-x}As$, with a transport mean free path approaching 0.1 mm in the best material. This has stimulated the development of quantum-mechanical devices that exploit the wave-like nature of electrons rather than their particle-like nature [1]. Many have ancestors in microwaves, such as the stub tuner, while others like the Aharonov-Bohm ring rely on the coupling between electron waves and external electromagnetic fields.

The building block of these devices is an 'electron waveguide' or 'quantum wire' in which the electrons in a 2DEG are further confined so that they remain free in one dimension only. The most versatile wires use the electrostatic potential from a split gate on the surface to confine the electrons [2]; see Fig. 1. Applying a negative bias to the gate depletes the regions beneath, leaving a narrow channel of electrons under the slit. Increasing the bias narrows the channel and, as in electromagnetic waveguides, reduces the number of modes that propagate, ideally to one. There is a long-standing prediction by Sakaki from simple scattering theory [3] that the transport mean free path should rise when a 2DEG is confined to a wire, confirmed by more recent analytic calculations [4,5].

Unfortunately, real devices have not met these expectations. An example that we shall discuss in detail below is the quantized conductance of a short wire — a constriction or "quantum point contact" (QPC). This works well in constrictions 0.2 μm long, but breaks down when the length is increased to 0.6 μm [6] — an order of magnitude below the transport mean free path. This is the opposite of Sakaki's prediction, and shows that there must be much stronger scattering in a patterned 2DEG than the transport mean free path of an unconfined 2DEG would lead us to believe.

Our modelling [4,7,8] has shown that the ionized donors in heterostructures create a strong random potential. Its long-ranged nature reduces its effect on the mobility of an unpatterned 2DEG but this changes in a waveguide, and there is strong scattering even in well-quantized point contacts. Back-scattering is needed to destroy quantization, and is provided by resonances trapped in bulges. This is a multiple-scattering process which is not included in the Born approximation, a vital ingredient of traditional

device modelling. The characteristics differ between devices, reflecting the precise configuration of impurities, so one cannot usefully simulate a "typical" device. These features are not unique to quantum-mechanical devices, and have been seen and modeled in a short-gate MODFET [9,10].

2. MODEL

Our model is illustrated in Fig. 1. This material is δ-doped, with the donors restricted to an atomic plane; a thick layer makes no significant difference. The material used in the experiments which we have modeled [6] had $c = 30$ nm, $s = 42$ nm and $N_D^{(2D)} = 4 \times 10^{16}$ m^{-2}. The structure divides naturally into three planes: surface, donors and 2DEG.

2.1 Surface

Part of the surface is covered by a metal gate and the rest is exposed GaAs. We assume that the surface states on the exposed surface remain perfectly pinned to E_F in the 2DEG, while those under the gate are pinned to the metal. Thus the surface behaves as an equipotential in the absence of a gate bias. This is convenient and consistent with the usual models for GaAs devices at room temperature. Unfortunately it is difficult to believe that the surface stays in equilibrium with the 2DEG at low temperature, because charge must move from the 2DEG to the surface states to maintain the equipotential. It may be more accurate to assume that the surface charge is frozen at low temperature; this is now being investigated.

2.2 Donors

We assume that the donors are fully ionized, but this gave too many electrons in the 2DEG using 4×10^{16} m^{-2} donors as grown. We corrected this problem, due to deep levels, by reducing the donors to 2.5×10^{16} m^{-2} which gave a density of electrons comparable with experiment, about 3×10^{15} m^{-2}. There are far fewer electrons in the 2DEG than ionized donors because most of the electrons from the donors are absorbed by the surface states. We also assume that the donors are randomly positioned, but Efros [11] has argued that there is strong correlation between the positions of *ionized* donors, although the donors as a whole are random in space. This could have a major effect on long-ranged fluctuations, which are responsible for many of the effects described below; we plan to investigate this. The potential from the donors is obtained simply by summing over a specific configuration of the discrete random ions, including an image to satisfy the boundary condition that E_F on the surface is pinned:

$$\phi_{\text{donors}}(\mathbf{r}) = \frac{e}{4\pi\varepsilon\varepsilon_0} \sum_{\text{donors},j} \left[\frac{1}{\sqrt{|\mathbf{r}-\mathbf{r}_j|^2 + s^2}} - \frac{1}{\sqrt{|\mathbf{r}-\mathbf{r}_j|^2 + (s+2c)^2}} \right] \tag{1}$$

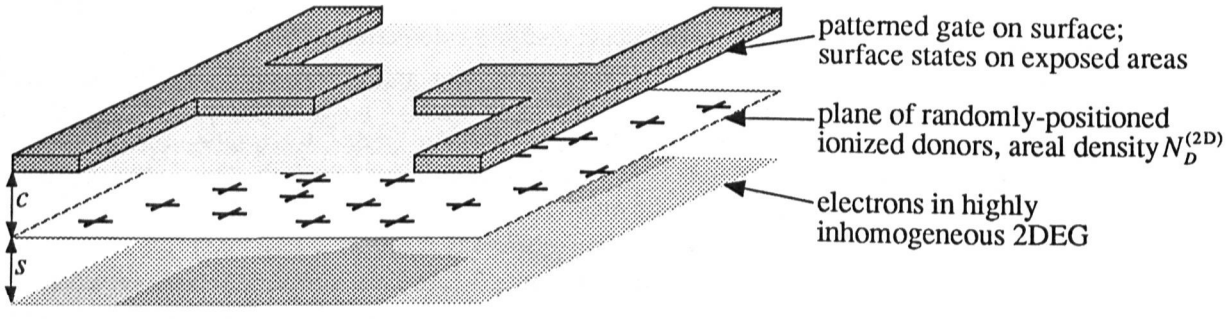

FIG. 1. Simplified model of a QPC showing the three planes of gate, donors and electrons.

2.3 Electrons

We assume that only one subband is occupied in the 2DEG, so that the density of states is a simple step, and use a local Thomas-Fermi model for the density of electrons:

$$n(\mathbf{r}) = \frac{m}{\pi\hbar^2}\left(E_F - E_c(\mathbf{r})\right)\Theta\left(E_F - E_c(\mathbf{r})\right) \tag{2}$$

where the Fermi energy E_F is assumed constant throughout, and $E_c(\mathbf{r})$ is the bottom of the conduction band at $\mathbf{r}$. This should be accurate provided that $E_c(\mathbf{r})$ varies slowly on the scale of the Fermi wavelength. While this is generally true, there are a few cases like resonances in which it fails.

2.4 Numerical method

Numerical methods are needed because wires have strongly inhomogeneous 2DEGs, whose screening cannot be treated analytically. We modeled a region about 1.5 μm square. Donors are thrown in at random, their coulomb energies are summed as in Eq. (1), and the potential from the gate is added to give the bare potential. Electrons are then added to the 2DEG according to the Thomas-Fermi model (Eq. 2), Poisson's equation is solved and the result added to the bare potential to give the total potential. This is used to generate another electron density and the loop is repeated to self-consistency with simple under-relaxation. The solution of Poisson's equation is needed only in the plane of the 2DEG, so we integrated it rather than solving the differential equation over the whole sample. As well as being faster, this method has the advantage that the boundary conditions are incorporated exactly. Periodic lateral boundary conditions turn the integrals into convolutions which were evaluated efficiently with fast Fourier transforms. The whole process must be repeated to self-consistency for each gate voltage and for several configurations of donors. We next find the conductance G using quantum mechanics; no additional scattering (phonons etc.) is included. Perfect leads are attached to the system by extending the potential profile at the left and right-hand edges outwards to infinity. The recursive Green's function method [12–14] then builds up the system in slices from left to right and yields G.

3. SELF-CONSISTENT POTENTIALS

Examples of the self-consistent density of electrons in the 2DEG are shown in Fig. 2. The dimensions of the devices match the experiments [6]. Fig. 2(a) shows the smooth potential obtained by smearing the donors into a sheet of uniform charge density, the usual procedure in modelling. The gate is 0.2 μm long, with a saddle-point potential in the 2DEG. Discrete random donors are included in Fig 2(b). The disorder is obvious! — heterojunctions are not as clean as one would like to believe. The fluctuations have a standard deviation $\sigma \approx 2$ meV, a significant fraction of $E_F \approx 10$ meV; $\sigma \approx 17$ meV where there are no electrons and therefore no screening.

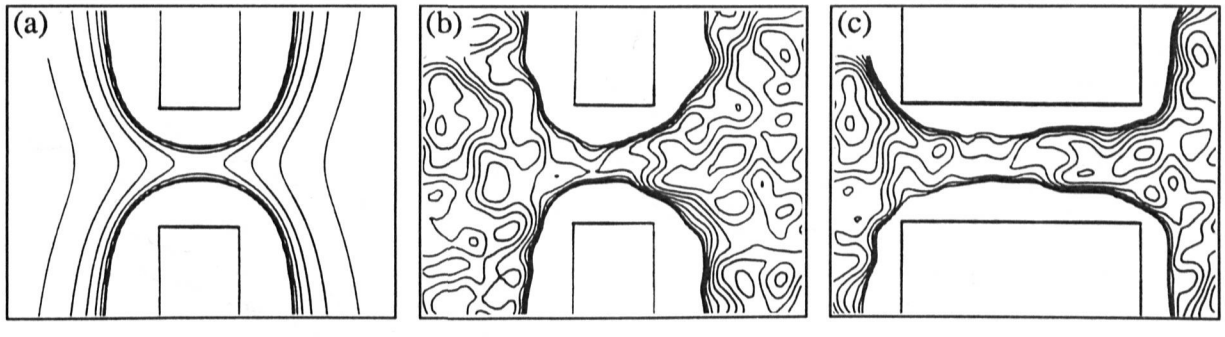

FIG. 2. Gate pattern on surface and density of electrons in 2DEG for regions 1.0×0.8 μm around three QPCs with a 0.3 μm gap between the gates. Contours start from zero and are 4.2×10^{14} m^{-2} apart (equivalent to 1.5 meV in energy). (a) gate 0.2 μm long with smooth potential; (b) 0.2 μm gate with discrete random donors; (c) 0.6 μm gate with random donors.

An important feature is the long range of the fluctuations, with a length scale of 0.2 μm; there are far fewer features in the potential than there are donors in the region (about 20,000). This is why the mean free path remains so long, about ten times the size of the region shown, because there is very little weight for back-scattering which requires a length scale of $\lambda_F/2 \approx 25\,\text{nm}$. The active region of the 0.2 μm QPC is comparable in area with the fluctuations and in this case is only slightly distorted. In contrast, Fig. 2(c) shows a QPC with a gate 0.6 μm long. This exceeds the length of the fluctuations and the potential in the "neck" is greatly distorted, which will lead to strong scattering of electrons. The potential gets rougher as the channel is squeezed further and the density of electrons is reduced, as seen before in wires [7].

4. TRANSPORT THROUGH A QUANTUM POINT CONTACT

4.1 Quantized conductance

It was found experimentally that the conductance of a QPC is quantized in steps of $2e^2/h$ [15,16]. The basic explanation was given in the original papers. Consider a 1D system at zero temperature, with a voltage V applied between two reservoirs. The current I is given by (density of active electrons) $\times$ (velocity) $\times$ (transmission coefficient). The density of active electrons is $\frac{1}{2}n_{1D}(E_F)eV$, where the $\frac{1}{2}$ selects one direction of motion, and the density of states at the Fermi energy is $n_{1D}(E_F) = 4/hv(E_F)$. Thus the velocity cancels with the density of states, the crucial feature, and the conductance $G = I/V = (2e^2/h)T(E_F)$. Each transverse mode can be treated separately in a perfect multimode system, and $G = (2e^2/h)n_{\text{modes}}$. Decreasing the bias on the QPC from cutoff increases the width of the constriction, allowing more modes to propagate, and a step in G occurs for each newly allowed mode. This simple theory has been confirmed by numerical simulations of model potentials (see, for example, [17–20]).

4.2 Numerical results

The calculated conductances $G(V_g)$ are plotted in Fig. 3 for several configurations of the random donors [8]. Curve A in Fig. 3(a) shows the good quantization of the smooth system with a 0.2 μm gate. Curve B shows that G can remain well quantized even in the presence of the random potential, although the steps between plateaus are broadened because the electrons' longitudinal velocity is low at the onset of a new mode and they are easily back-scattered. Another sample, not shown, also has good quantization. Curves C and D, for two other configurations, are poorly quantized with structure due to the random potential. For the 0.6 μm point contact in Fig. 3(b), the smooth potential shows better quantization than the shorter point contact because tunnelling through the saddle point is reduced (curve A). Including the random potential reverses this, and quantization is much worse than in the shorter device (curves B–D). No sample shows more than one good plateau because of back-scattering by the random potential in the constriction. Typically there is almost no remnant of the steps, in agreement with experiment [6].

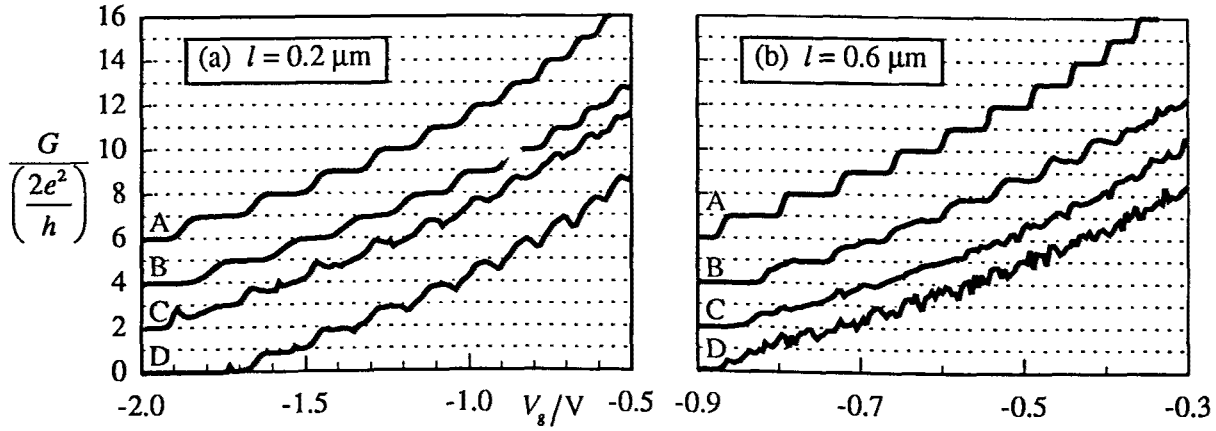

FIG. 3. Calculated conductance as a function of gate voltage for several QPCs with gates of length 0.2 μm and 0.6 μm.

Specific features in the random potential can be identified. Curve D in Fig. 3(a) shows sharp peaks in $G(V_g)$ below the onset of the first and second plateaus, a signature of resonant tunneling, and the potential has a clear double barrier in the QPC [8]. The resonance broadens and disrupts the higher plateaus: resonant tunnelling turns into resonant back-scattering as discussed below. Similar resonances have been seen in calculations with short-ranged attractive potentials [21,22]. Features in the potential can be explored experimentally by scanning the point contact with a differential bias [23–25].

4.3 Analysis of scattering

These results have shown that the random potential from the ionized donors destroy the quantized conductance on the length scale observed experimentally, but do not yet explain why scattering is so strong. We performed a modal analysis of transport in the constriction to investigate this [4]. Briefly, the idea is to expand the wavefunction in the form

$$\psi(x,y) = \sum_n \left\{ c_n^+(x) \exp\left[ik_n(x)x\right] + c_n^-(x) \exp\left[-ik_n(x)x\right] \right\} \phi_n(y;x), \tag{2}$$

where $\phi_n(y;x)$ are the *local* transverse modes of the waveguide, solutions of the 1D Schrödinger equation in y for a slice through the potential at a particular value of the longitudinal coordinate x. This form for ψ can then be substituted into the full 2D Schrödinger equation and the $\phi_n(y;x)$ integrated out to leave a set of coupled-mode equations for the coefficients $c_n^{\pm}(x)$, the amplitudes of the modes.

A useful simplification is to neglect the inter-mode coupling and assume that each mode propagates independently, the "adiabatic approximation" [26]. Our numerical results, using the potentials described in the previous section, show that disorder renders this approximation invalid; electrons scatter rapidly from one mode to another even in a well-quantized device. The mean free path, about 0.1 μm, agrees closely with the Born approximation. The conductance is unaffected because scattering is predominantly *forward*: the magnitude of the velocity changes but not its sign. This dominant low-angle scattering is characteristic of a slowly-varying potential [27].

This leaves the question: how can back-scattering, which is needed to decrease the conductance, be produced by such a slowly-varying potential? We find that resonances trapped in bulges in the constriction cause strong back-scattering and produce the dips seen in $G(V_g)$ seen in Fig. 3, destroying quantization. They can also cause peaks in the conductance, as we saw earlier. The behavior depends on the way in which electrons enter the resonance: the conductance rises if they enter by tunnelling, but decreases if they enter by scattering. Tunnelling is the only mechanism possible when there are no conducting modes, giving a peak in $G(V_g)$, but scattering becomes more probable as the number of conducting modes rises and the peak turns into a dip. This is illustrated beautifully by curve D in Fig. 3(b). The effect of model resonances in narrow channels has been investigated extensively [28]. It is known theoretically that scattering events cannot be treated as independent in 1D [29] and the resonant back-scattering process provides a clear physical demonstration of this, explaining why Sakaki's prediction [3] fails. The maximum length of a good QPC will be set by the correlation length of the random potential, rather than a conventional mean free path, if resonances are the dominant back-scattering mechanism; this is about 0.2 μm for our potentials. Resonances are particularly important in the wires that we have studied because the random potential is larger than the separation between subbands. The picture might be very different if the opposite were the case, and we intend to explore this.

5. DISCUSSION AND CONCLUSIONS

We have shown that the 2DEG feels a large, but slowly-varying, random potential even in high-quality heterostructures. It is not apparent in the mobility of an unpatterned 2DEG but causes strong scattering in a quantum wire, reducing the mean free path drastically. This presents a major obstacle to the development of quantum devices based on waveguides. There can be large variations between devices and the usual assumption of independent scattering events fails badly in quasi-1D systems; both of these results mean that conventional Monte Carlo methods are inapplicable to these systems.

It has long been predicted that the discrete nature of donors would lead to fluctuations in the threshold voltage and other parameters between devices as their size is reduced [30–32]. Our results are more dramatic, because the randomness destroys the operation of the device. One reason is that there are no electrons immediately around the ionized donors to screen them in a heterostructure. This enhances the fluctuations, as found in planar-doped barriers [33]. The outlook for very small devices based on current heterostructures therefore looks gloomy. Fortunately there is experimental evidence to the contrary: quantized conductance has been observed in wet-etched wires 10 μm long [34]. Although there is evidence that our simulations overestimate the randomness, possibly because the donors are correlated [11], this experiment is inexplicable within our current picture. Much work clearly remains before our understanding of heterostructures and quasi-one-dimensional systems can be considered complete.

Acknowledgments

The U.K. SERC supported the work at Glasgow, where we would like to acknowledge our collaborators J. R. Barker and J. M. Arnold. JHD is grateful to the U.S. ONR for additional support. It is a pleasure to thank D. P. Monroe for discussions concerning the ionization of dopant inpurities, as well as our many experimental colleagues whose results have driven this work.

REFERENCES

1. W. P. Kirk and M. A. Reed, *Proc. Int. Symp. on Nanostructures and Mesoscopic Systems*, Academic, Boston (1991).
2. T. J. Thornton, M. Pepper, H. Ahmed, D. Andrews and G. J. Davies, *Phys. Rev. Lett.*, **56**, 1198 (1986).
3. H. Sakaki, *Jap. Jnl. Appl. Phys.*, **19**, L735 (1980).
4. M. J. Laughton, J. R. Barker, J. A. Nixon and J. H. Davies, *Phys. Rev. B*, **44**, 1150 (1991).
5. L. I. Glazman and M. Jonson, *Phys. Rev. B*, **44**, 15 (1991).
6. G. Timp, R. Behringer, S. Sampere, J. E. Cunningham and R. E. Howard, in *Proc. Int. Symp. on Nanostructure Physics and Fabrication*, College Station, Texas, ed. M. A. Reed and W. P. Kirk, p. 331, Academic Press (1989).
7. J. A. Nixon and J. H. Davies, *Phys. Rev. B*, **41**, 7929 (1990).
8. J. A. Nixon, J. H. Davies and H. U. Baranger, *Phys. Rev. B*, **43**, 12638 (1991).
9. S. Washburn, A. B. Fowler, H. Schmid and D. Kern, *Phys. Rev. B*, **38**, 1554 (1988).
10. J. H. Davies and J. A. Nixon, *Phys. Rev. B*, **39**, 3423 (1989).
11. A. L. Efros, F. G. Pikus and G. G. Samsonidze, *Phys. Rev. B*, **41**, 8295 (1990); D. P. Monroe, unpublished.
12. D. J. Thouless and S. Kirkpatrick, *J. Phys. C*, **14**, 235 (1981).
13. P. A. Lee and D. S. Fisher, *Phys. Rev. Lett.*, **47**, 882 (1981).
14. A. MacKinnon, *Z. Phys. B*, **59**, 385 (1985).
15. D. A. Wharam, T. J. Thornton, R. Newbury, M. Pepper, H. Ahmed, J. E. Frost, D. G. Hasko, D. C. Peacock, D. A. Ritchie and G. A. C. Jones, *J. Phys. C*, **21**, L209 (1988).
16. B. J. van Wees, H. van Houten, C. W. J. Beenakker, J. G. Williamson, L. P. Kouwenhoven, D. van der Marel and C. T. Foxon, *Phys. Rev. Lett.*, **60**, 848 (1988).
17. A. Szafer and A. D. Stone, *Phys. Rev. Lett.*, **62**, 300 (1989).
18. G. Kirczenow, *Solid State Commun.*, **68**, 715 (1988).
19. E. G. Haanappel and D. van der Marel, *Phys. Rev. B*, **39**, 5484 (1989).
20. E. Tekman and S. Ciraci, *Phys. Rev. B*, **42**, 9098 (1990).
21. C. S. Chu and R. S. Sorbello, *Phys. Rev. B*, **40**, 5941 (1989).
22. P. F. Bagwell, *Phys Rev B*, **41**, 10354 (1990).
23. L. I. Glazman and I. A. Larkin, *Semicond. Sci. Technol.*, **6**, 32 (1991).
24. J. G. Williamson, C. E. Timmering, C. J. P. M. Harmans, J. J. Harris and C. T. Foxon, *Phys Rev B*, **42**, 7675 (1990).
25. C. C. Eugster and J. A. del Alamo, *Phys. Rev. Lett.*, **64**, 3586 (1991).
26. L. I. Glazman, G. B. Lesovick, D. E. Khmel'nitskii and R. I. Shekhter, *JETP Letters*, **48**, 238 (1988).
27. S. Das Sarma and F. Stern, *Phys. Rev. B*, **32**, 8442 (1988).
28. A. Kumar and P. F. Bagwell, *Phys. Rev. B*, **43**, 9012 (1991).
29. A. A. Abrikosov and I. A. Ryzhkin, *Sov. Phys. JETP*, **44**, 630 (1976).
30. R. W. Keyes, *IEEE J. Solid-state circuits*, **10**, 245 (1975).
31. R. Landauer, in *Electrical transport and optical properties of inhomogeneous media*, ed. J. C. Garland and D. B. Tanner, p. 2, AIP (1978).
32. W. J. Boudville and T. C. McGill, *Appl. Phys. Lett.*, **48**, 791 (1986).
33. D. Arnold and K. Hess, *J. Appl. Phys.*, **61**, 5178 (1987).
34. K. Ismail, S. Washburn and K. Y. Lee, *Appl. Phys. Lett.*, **59**, 1998 (1992).